



HAL
open science

Cumulative effects of electrode and dielectric surface modifications on pentacene-based transistors

Mélanie Devynck, Pascal Tardy, Guillaume Wantz, Yohann Nicolas, Luc Vellutini, Christine Labrugère, Lionel Hirsch

► **To cite this version:**

Mélanie Devynck, Pascal Tardy, Guillaume Wantz, Yohann Nicolas, Luc Vellutini, et al.. Cumulative effects of electrode and dielectric surface modifications on pentacene-based transistors. *Applied Physics Letters*, 2012, 100 (5), pp.053308. 10.1063/1.3681791 . hal-00670178

HAL Id: hal-00670178

<https://hal.science/hal-00670178v1>

Submitted on 26 Mar 2024

HAL is a multi-disciplinary open access archive for the deposit and dissemination of scientific research documents, whether they are published or not. The documents may come from teaching and research institutions in France or abroad, or from public or private research centers.

L'archive ouverte pluridisciplinaire **HAL**, est destinée au dépôt et à la diffusion de documents scientifiques de niveau recherche, publiés ou non, émanant des établissements d'enseignement et de recherche français ou étrangers, des laboratoires publics ou privés.

RESEARCH ARTICLE | FEBRUARY 03 2012

Cumulative effects of electrode and dielectric surface modifications on pentacene-based transistors

Mélanie Devynck; Pascal Tardy; Guillaume Wantz; Yohann Nicolas; Luc Vellutini; Christine Labrugère; Lionel Hirsch



Appl. Phys. Lett. 100, 053308 (2012)

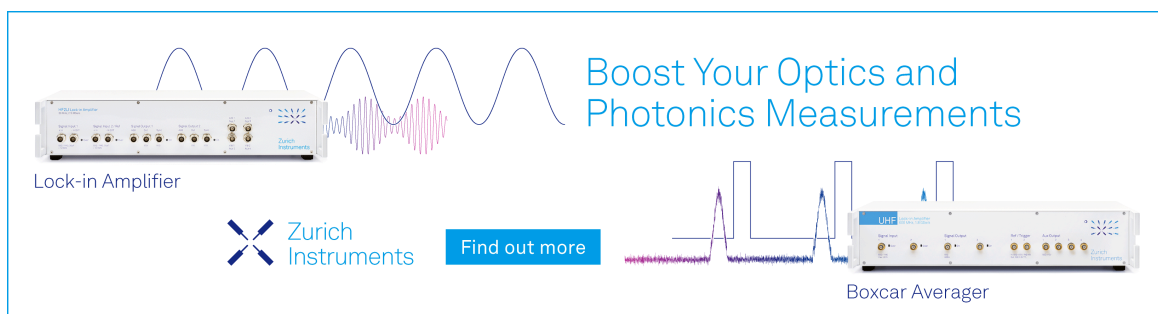
<https://doi.org/10.1063/1.3681791>



View Online



Export Citation



Boost Your Optics and Photonics Measurements

Lock-in Amplifier

Zurich Instruments

Find out more

Boxcar Averager

Cumulative effects of electrode and dielectric surface modifications on pentacene-based transistors

Mélanie Devynck,¹ Pascal Tardy,¹ Guillaume Wantz,¹ Yohann Nicolas,² Luc Vellutini,² Christine Labrugère,³ and Lionel Hirsch^{1,a)}

¹Univ. Bordeaux, IMS, UMR 5218, F-33400 Talence, France and CNRS, IMS, UMR 5218, F-33400 Talence, France

²Univ. Bordeaux, ISM, UMR 5255, F-33400 Talence, France and CNRS, ISM, UMR 5255, F-33400 Talence, France

³Univ. Bordeaux, ICMCB, UPR 9048, F-33600 Pessac, France and CNRS, ICMCB, UPR 9048, F-33600 Pessac, France

(Received 5 January 2012; accepted 13 January 2012; published online 3 February 2012)

Surface modifications of the dielectric and the metal of pentacene-based field effect transistors using self-assembled monolayer (SAM) were studied. First, a low interfacial trap density and pentacene 2D-growth were favored by the nonpolar and low surface energy of octadecyltrichlorosilane-based SAM. This treatment led to increased mobility up to $0.4 \text{ cm}^2 \text{ V}^{-1} \text{ s}^{-1}$ and no observable hysteresis on transfer curves. Second, reduced hole injection barrier and contact resistance were achieved by fluorinated thiols deposited on gold contacts resulting in an increased mobility up to $0.6 \text{ cm}^2 \text{ V}^{-1} \text{ s}^{-1}$. Finally, a high mobility of $2.6 \text{ cm}^2 \text{ V}^{-1} \text{ s}^{-1}$ was achieved by cumulative effects of both treatments. © 2012 American Institute of Physics. [doi:10.1063/1.3681791]

The performances of organic field-effect transistors (OFETs) are strongly related to the charge carriers injection from contacts and to their transport in the first organic semiconductor (OSC) monolayers close to the dielectric interface.^{1–3} Indeed, charge transport is affected by the OSC thin film morphology and by the density of interfacial traps depending on the topologic roughness^{4,5} and/or on the “energetic roughness” due to surface dipoles.^{6,7} Furthermore, in the case of bottom gate device architecture, the dielectric surface energy and roughness influence the growth of OSC layers. For instance, for a sublimated pentacene-based polycrystalline film, a high surface energy or a rough surface results in 3D small grains and in high density of grain boundaries associated to charge traps.⁸ Thereby, in order to improve OFETs performances, a very close look at the dielectric surface properties should be taken. These properties can be modified by various self assembled monolayer (SAM) using compounds with phosphonic acid⁹ head groups on Al_2O_3 , hexamethyldisilazane (HMDS),¹⁰ or trichlorosilane derivatives^{11,12} on SiO_2 , in order to prevent the formation of trapping sites and promote a 2D OSC growth.¹³ Another limitation of OFETs performances is due to the contact resistance (R_C) at the OSC/metal interface, which restricts the charge injection or extraction. R_C increases with the mismatch of the metal Fermi level and either the highest occupied molecular orbital level (HOMO) or the lowest unoccupied molecular orbital level (LUMO) of the OSC, which induces an energetic barrier.^{14,15} Moreover, charge injection is influenced by the tunneling barrier width modulated by alkyl chain length and by the work function related to the local dipole moment. In case of pentacene-based OFETs, the hole injection barrier (HIB), i.e., the difference

between the pentacene HOMO level and the metal Fermi level, can be reduced by increasing the metal work function. Previous works have already demonstrated that a modification of gold contacts with fluorinated thiol SAMs reduced the HIB by an increase of metal work function induced by a charge redistribution at metal surface.^{16–19}

In the present work, the influence of both SiO_2 and gold electrodes treatments on pentacene-based OFETs performances (effective mobility μ_e , I_{on}/I_{off} ratio, hysteresis) has been studied. In a first part, octadecyltrichlorosilane (OTS) was grafted on SiO_2 surface. The modifications induced on the surface energy were measured by contact angle measurements and linked to the OSC thin film morphology investigated by AFM. In a second part, the electrode surface was modified by three fluorinated thiols: pentafluorobenzenethiol (PFBT), nonafluoro-1-hexanethiol or 1H,1H,2H,2H-perfluorohexanethiol ($\text{CF}_3(\text{CF}_2)_3\text{CH}_2\text{CH}_2\text{SH}$, named PFHT), and heptadecafluoro-1-decanethiol or 1H,1H,2H,2H-perfluorodecanethiol ($\text{CF}_3(\text{CF}_2)_7\text{CH}_2\text{CH}_2\text{SH}$, named PFDT) (see Fig. 2(c)). The influence of fluorinated thiols SAMs on the electrode work function was controlled by UV photoemission spectroscopy (UPS). For each electrode treatment, R_C was extracted using the transfer line method (TLM).²⁰ Finally, highest mobilities were achieved with both interfaces modifications.

OFETs devices were fabricated in a bottom gate bottom contact geometry with commercial substrates purchased from *Fraunhofer IPMS* consisting of heavily doped Si wafer featuring a 230 nm SiO_2 layer with patterned (30 nm thickness) Au electrodes on a 10 nm ITO adhesion layer. The electrodes set involved different channel lengths ($L = 2.5, 5, 10, \text{ and } 20 \mu\text{m}$) and 1 cm width (W). Substrates were rinsed with acetone, isopropanol followed by UV-ozone cleaning for 20 min. Prior to every SAMs grafting process, commercially available OTS (*Aldrich*) was purified by distillation at 220 °C under vacuum. The OTS-based SAMs were formed

^{a)}Author to whom correspondence should be addressed. Electronic mail: lionel.hirsch@ims-bordeaux.fr.

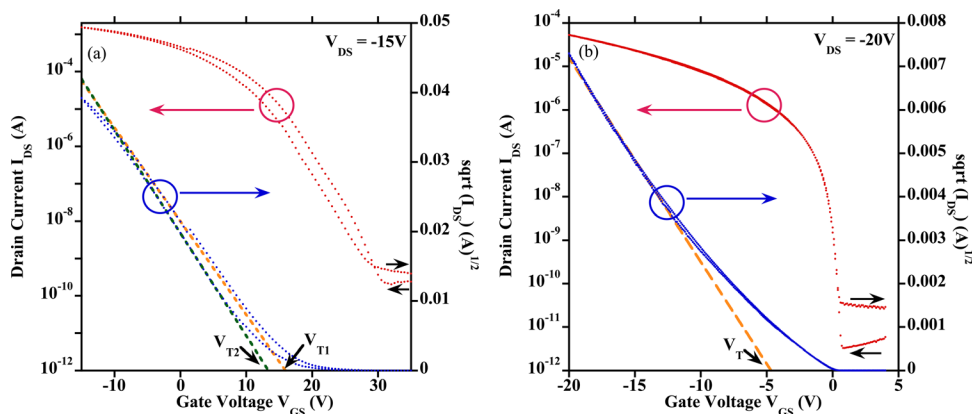


FIG. 1. (Color online) Transfer characteristics I_{DS} - V_{GS} for OFETs depending on the dielectric treatment. For non treated OFETs (a), a shift in the threshold voltage in I_{DS} - V_{GS} curves, i.e., an hysteresis, of $3\text{ V}(V_{T1}-V_{T2})$ can be noticed. This effect is not observed for OTS pretreated OFETs (b).

by immersing the silicon wafers in a 2.5 mM cyclohexane:chloroform solution (70:30 v/v) (Aldrich, $\text{H}_2\text{O} < 0.01\%$) for 1 h at 20°C under argon atmosphere.²¹ After the formation of the SAMs, the wafers were rinsed with the same solvents as the one used for deposition. The surface energies of SiO_2 and OTS were determined using a KRUSS DSA 100 goniometer by the method proposed by Owens and Wendt (Eq. (1))²² based on the contact angle measurements of different liquids on the substrate surface at 20°C in static mode.

$$\gamma_{SL} = \gamma_S + \gamma_L + 2 \left(\sqrt{\gamma_L^d \gamma_S^d} + \sqrt{\gamma_L^p \gamma_S^p} \right). \quad (1)$$

In our experiments each surface was probed with three test liquids. Ultrapure water (a very polar liquid), diiodomethane (a very nonpolar liquid), and ethyleneglycol were chosen due to their wide range of surface tensions and ratios of dispersive-to-polar components. The values of surface tensions (γ_L), their polar components (γ_L^p), and dispersive components (γ_L^d) are listed as following: ultrapure water ($\gamma_L = 72.8 \text{ mN m}^{-1}$, $\gamma_L^p = 51 \text{ mN m}^{-1}$, $\gamma_L^d = 21.8 \text{ mN m}^{-1}$), diiodomethane ($\gamma_L = 50.8 \text{ mN m}^{-1}$, $\gamma_L^p = 0 \text{ mN m}^{-1}$, $\gamma_L^d = 50.8 \text{ mN m}^{-1}$), and ethyleneglycol ($\gamma_L = 48.3 \text{ mN m}^{-1}$, $\gamma_L^p = 19 \text{ mN m}^{-1}$, $\gamma_L^d = 29.3 \text{ mN m}^{-1}$). In case of electrode treatment, the SAM depositions were performed by immersing the substrates into a 3 mM solution of fluorinated PFHT or PFDT in absolute ethanol ($\text{H}_2\text{O} < 0.2\%$) for 48 h¹⁸ or into a 10 mM solution of PFBT in anhydrous toluene ($\text{H}_2\text{O} < 0.005\%$) for 2 min.²³ Wafers were then rinsed with the same solvent as the one used for deposition. Pentacene was then vacuum evaporated (1×10^{-6} mbar) at a rate of 0.1 \AA/s to a total thickness of 30 nm in a temperature-controlled alumina-based crucible. The transfer I_{DS} - V_{GS} curves of transistors were measured with a semiconductor analyzer Keithley 4200 on a triaxial connected probe station in a dry nitrogen glove box (O_2 and

$\text{H}_2\text{O} < 1 \text{ ppm}$). In order to investigate the effect of the dielectric surface treatment on the density of grain boundaries in the first OSC layers responsible for charge transport limitation, the surface morphology of a 3 nm-thick pentacene layer deposited on the dielectric surface (bare SiO_2 or OTS-modified SiO_2) was studied by AFM (Veeco 3100, Digital Instrument) measurements. For UPS measurement, fluorinated thiols SAMs and a 15 nm-thick pentacene layer were deposited as described above on a 150 nm-thick Au layer. UPS was performed using instruments and experimental methods that have been described in details elsewhere.²⁴ The instrument resolution during data collection was 0.1 eV.

SiO_2 -based OFETs and the OTS-modified OFETs were electrically characterized and their performances were determined in saturation regime and summarized in Table I. The normalized standard deviation (NSD) was calculated according to Eq. (2)

$$NSD(x) = \frac{SD(x)}{\bar{x}} = \frac{\sqrt{\frac{1}{n-1} \sum (x_i - \bar{x})^2}}{\bar{x}}. \quad (2)$$

A significant increase of the hole mobility along with a decrease of the threshold voltage, from 8.9 V (bare SiO_2) to -1.8 V , was observed in case of OTS-pretreated OFETs. The reduction of V_T can be attributed to a lower concentration of trap states at the dielectric surface. Moreover, the hysteresis (the difference in transfer curves when sweeping V_{GS} back and forth), that is detrimental for the conception of OFETs based circuits, completely disappeared in the case of OTS-treated OFETs (Fig. 1). As hysteresis in SiO_2 based OFETs is well-known to be due to the SiO_2 surface trap states,²⁵⁻²⁹ this behavior suggests that charge trapping/de-trapping effects at the pentacene/dielectric interface were significantly attenuated by the OTS surface modification.

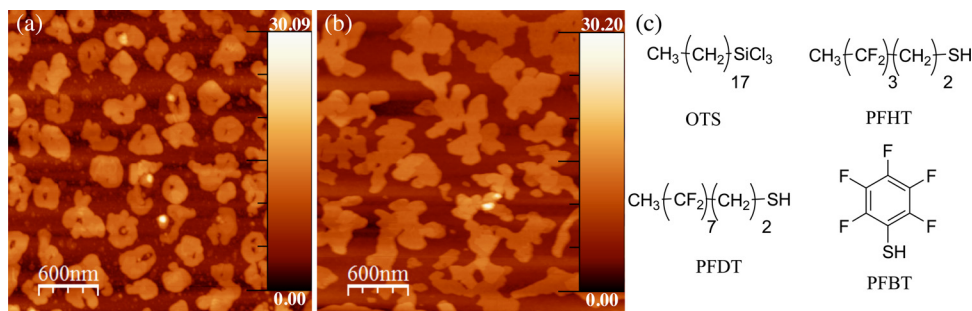


FIG. 2. (Color online) AFM images (topography) of 3 nm pentacene deposited on (a) SiO_2 and (b) OTS surface. The scanned area is $3 \mu\text{m} \times 3 \mu\text{m}$; vertical scale is given in nm. (c) Molecular structures of the SAMs used to modify either the dielectric or the electrode surfaces.

TABLE I. Electrical performances of pentacene-based OFETs depending on dielectric and/or on electrode treatment. The values shown are averaged over ~ 20 devices for each surface treatment. The NSD was determined as described in the Eq. (2). The HIB corresponds to the difference between the electrode Fermi level and the pentacene HOMO level (calculated at 5.5 eV).

Dielectric modification	Electrode modification	Average mobility μ_e ($\text{cm}^2 \cdot \text{V}^{-1} \cdot \text{s}^{-1}$) (NSD) Highest mobility	Average I_{on}/I_{off}	R_C @ $V_G = -10$ V (k Ω)	Electrode work function (HIB) (eV)
–	–	0.1 (0.7) 0.2	1.9×10^6	9.6	4.9 (0.6)
OTS	–	0.4 (0.2) 0.5	1.7×10^8	2.5	
–	PFBT	0.4 (0.3) 0.6	1.4×10^5	2.7	5.4 (0.1)
–	PFHT	0.3 (0.3) 0.4	9.8×10^4	3.8	5.1 (0.4)
–	PFDT	0.2 (0.5) 0.3	5.8×10^5	11.5	5.7 (0.2)
OTS	PFBT	1.3 (0.6) 2.6	1.7×10^7	5.1	

These traps states can arise in the OSC layer either from dipole disorder at the dielectric interface mainly due to the hydrophilic character of SiO_2 surface causing adsorption of water molecules at the interface, or from grain boundaries resulting from crystallographic defects³⁰ due to high surface energy of dielectric^{31,32} and rough surfaces.^{4,5} Therefore, SiO_2 and OTS surface energies were determined by contact angle measurement while the roughness was measured by AFM. Although the SiO_2 surface was initially quite smooth (rms value = 0.4 nm), OTS treatment further reduced the dielectric roughness by a factor 2 (rms value = 0.2 nm).³³ Additionally, OTS modification yielded to a drastic reduction of the polar component of the SiO_2 surface energy from 37 mN m^{-1} to a value close to 0 mN m^{-1} (Table II). Consequently, nonpolar and hydrophobic OTS surface could efficiently shield pentacene from most of the energetic disorder at the SiO_2 surface and prevent adsorption of water molecules explaining the absence of hysteresis. The influence of the SiO_2 treatment on the pentacene growth is presented on Fig. 2. Whereas the mismatch between the surface energies of pentacene and SiO_2 induced a small grains 3D growth (diameter ~ 200 nm) resulting in a discontinuous film with a high density of grain boundaries, larger 2D grains (diameter ~ 700 nm) were observed on OTS surface.

Besides, the electrode surfaces were modified by the fluorinated thiols PFBT, PFHT, PFDT, and the electrical characteristics of OFETs were summarized in Table I. As the field-effect mobility, μ_e is not only dependent on the charge transport in OSC but also on charge injection at the OSC/electrode interface, governed by R_C and HIBs, these aspects were investigated. R_C was extracted from the overall device resistance R_{on} measured by TLM according Eq. (3), with W the channel width, C the capacitance per area, V_T and V_{GS} the threshold and gate-source voltage, respectively. HIB was calculated as the difference between the metal work function of metal and the HOMO of pentacene (experimental value of 5.5 eV). The values of R_C and HIBs are reported in Table I.

TABLE II. Surface energy of the dielectric (OTS) surface modified. The surface energy of pentacene is 38.3 mN m^{-1} . The dispersion and polar components of the energy are 35.3 and 3.0 mN/m^{-1} , respectively.

	Surface energy γ_s ($\text{mN} \cdot \text{m}^{-1}$)	Polar component γ_s^p ($\text{mN} \cdot \text{m}^{-1}$)	Dispersive component γ_s^d ($\text{mN} \cdot \text{m}^{-1}$)
SiO_2	67.3 ± 3.4	37.3 ± 1.7	30.3 ± 1.7
OTS	25.6 ± 1.4	0.4 ± 0.2	25.2 ± 1.2

Concerning HIB, the calculated values are consistent with those reported in literature^{16,18}

$$\left. \frac{\partial V_{DS}}{\partial I_{DS}} \right|_{V_{DS}=0}^{V_{GS}} = R_{on} = R_{ch} + R_C = \frac{L}{WC\mu(V_G - V_T)} + R_C. \quad (3)$$

Despite of a non-linear correlation between the performances and the HIBs, the best mobilities were obtained for lower HIB values. Especially, for PFBT treatment, hole mobility was increased up to a factor 4, from 0.1 to 0.4 $\text{cm}^2 \text{V}^{-1} \text{s}^{-1}$, and I_{on}/I_{off} ratio was slightly improved. Considering the influence of R_C itself, the results in Table I show that, as expected, a decrease in R_C came along with a mobility increase. It is worth to mention that in case of PFDT treatment, R_C was increasing whereas the HIB was reduced. Beyond HIB values and as previously mentioned, R_C is governed by the tunneling barrier width linked to SAM thickness. Therefore, this surprising behavior could be attributed to the fact that the long PFDT alkyl chain, being composed of 10 carbons versus 6 in case of PFHT, could act as an insulating barrier.¹⁶ Finally, the device fabrication with cumulative treatments (OTS-treated SiO_2 and PFBT-treated electrodes) were realized and electrically characterized. With such interfaces modifications a mobility, averaged over 20 samples, of 1.3 $\text{cm}^2 \text{V}^{-1} \text{s}^{-1}$ have been obtained with a maximum of 2.6 $\text{cm}^2 \text{V}^{-1} \text{s}^{-1}$.

To conclude, OFETs performances were improved in different ways thanks to OTS treatment on SiO_2 combined with polar thiol SAMs on gold electrodes. The nonpolar alkyl chains greatly reduced the interfacial charge traps density resulting in a low threshold voltage and in an inexistent hysteresis. Moreover, the low surface energy and the smooth OTS surface favored a 2D growth and charge transport, which explained the higher mobility of up to 0.6 $\text{cm}^2 \text{V}^{-1} \text{s}^{-1}$. In case of electrode treatment, a decrease of the HIB and therefore a reduction of the R_C facilitating the charge injection were observed leading to higher mobilities up to 0.6 $\text{cm}^2 \text{V}^{-1} \text{s}^{-1}$. Finally, OFETs with a mobility of 2.6 $\text{cm}^2 \text{V}^{-1} \text{s}^{-1}$ have been obtained according to the cumulative effect of both surface treatments.

This work has been supported by the ANR through the HiLIGHT ANR-08-BLAN-0161-03 project and the R \ddot{O} gion Aquitaine through the OFET project. Authors gratefully thank Sokha Khiev for his technical contribution to this work.

- ¹M. Kiguchi, M. Nakayama, T. Shimada, and K. Saiki, *Phys. Rev. B* **71**, 1 (2005).
- ²F. Dinelli, M. Murgia, P. Levy, M. Cavallini, F. Biscarini, and D. De Leeuw, *Phys. Rev. Lett.* **92**, 90 (2004).
- ³G. Horowitz, P. Lang, W. Kalb, and M. Mottaghi, in *Proceedings of the International Symposium on Super-Functionality Organic Devices IPAP Conference Series* (The Institute of Pure and Applied Physics, Chiba, Japan, 2005), Vol. 6, pp. 125–129.
- ⁴S. Steudel, S. De Vusser, S. De Jonge, D. Janssen, S. Verlaak, J. Genoe, and P. Heremans, *Appl. Phys. Lett.* **85**, 4400 (2004).
- ⁵S. E. Fritz, T. W. Kelley, and C. D. Frisbie, *J. Phys. Chem. B* **109**, 10574 (2005).
- ⁶J. Veres, S. Ogier, G. Lloyd, and D. De Leeuw, *Chem. Mater.* **16**, 4543 (2004).
- ⁷J. Veres, S. D. Ogier, S. W. Leeming, D. C. Cupertino, and S. Mohialdin Khaffaf, *Adv. Funct. Mater.* **13**, 199 (2003).
- ⁸G. Horowitz, M. E. Hajlaoui, and R. Hajlaoui, *J. Appl. Phys.* **87**, 4456 (2000).
- ⁹I. G. Hill, C. M. Weinert, L. Kreplak, and B. P. Zyl, *Appl. Phys. A* **95**, 81 (2008).
- ¹⁰S. Y. Yang, K. Shin, and C. E. Park, *Adv. Funct. Mater.* **15**, 1806 (2005).
- ¹¹Y.-Y. Lin, D. J. Gundlach, S. F. Nelson, and T. N. Jackson, *IEEE Electron Device Lett.* **18**, 606 (1997).
- ¹²K. Suemori, S. Uemura, M. Yoshida, S. Hoshino, N. Takada, T. Kodzasa, and T. Kamata, *Appl. Phys. Lett.* **91**, 192112 (2007).
- ¹³S. Steudel, D. Janssen, S. Verlaak, J. Genoe, and P. Heremans, *Appl. Phys. Lett.* **85**, 5550 (2004).
- ¹⁴N. Koch, *Chem. Phys. Chem.* **8**, 1438 (2007).
- ¹⁵N. Koch, A. Kahn, J. Ghijsen, J.-J. Pireaux, J. Schwartz, R. L. Johnson, and A. Elschner, *Appl. Phys. Lett.* **82**, 70 (2003).
- ¹⁶P. Marmont, N. Battaglini, P. Lang, G. Horowitz, J. Hwang, A. Kahn, C. Amato, and P. Calas, *Org. Electron.* **9**, 419 (2008).
- ¹⁷I. H. Campbell, J. D. Kress, R. L. Martin, and D. L. Smith, *Appl. Phys.* **71**, 3528 (1997).
- ¹⁸B. De Boer, A. Hadipour, M. M. Mandoc, T. Van Woudenberg, and P. W. M. Blom, *Adv. Mater.* **17**, 621 (2005).
- ¹⁹K. Asadi, F. Gholamrezaie, E. C. P. Smits, P. W. M. Blom, and B. De Boer, *J. Mater. Chem.* **17**, 1947 (2007).
- ²⁰P. V. Necliudov, M. S. Shur, D. J. Gundlach, and T. N. Jackson, *Solid-State Electron.* **47**, 259 (2003).
- ²¹A. N. Parikh, D. L. Allara, I. B. Azouz, and F. Rondelez, *J. Phys. Chem.* **98**, 7577 (1994).
- ²²D. K. Owens and R. C. Wendt, *J. Appl. Polym. Sci.* **13**, 1741 (1969).
- ²³S. K. Park, T. N. Jackson, J. E. Anthony, and D. A. Mourey, *Appl. Phys. Lett.* **91**, 063514 (2007).
- ²⁴W. R. Salaneck, M. Logdlund, M. Fahlman, G. Greczynski, and T. Kugler, *Mater. Sci.* **34**, 121 (2001).
- ²⁵G. Gu, M. G. Kane, J. E. Doty, and A. H. Firester, *Appl. Phys. Lett.* **87**, 243512 (2005).
- ²⁶W. Kim, A. Javey, O. Vermesh, Q. Wang, Y. Li, and H. Dai, *Nano Lett.* **3**, 193 (2003).
- ²⁷S. Kim, H. Yang, S. Yang, K. Hong, D. Choi, C. Yang, D. Chung, and C. Park, *Org. Electron.* **9**, 673 (2008).
- ²⁸J. C. Ribierre, S. Ghosh, K. Takaishi, T. Muto, and T. Aoyama, *J. Phys. D* **44**, 205102 (2011).
- ²⁹G. Robert, V. Derycke, M. F. Goffman, S. Lenfant, D. Vuillaume, and J.-P. Bourgoin, *Appl. Phys. Lett.* **93**, 143117 (2008).
- ³⁰G. Horowitz and M.E. Hajlaoui, *Synth. Met.* **122**, 185 (2001).
- ³¹S. Y. Yang, K. Shin, and C. E. Park, *Adv. Funct. Mater.* **15**, 1806 (2005).
- ³²J. Park, J.-H. Bae, W.-H. Kim, S.-D. Lee, J. S. Gwag, D. W. Kim, J. C. Noh, and J. S. Choi, *Solid-State Electron.* **54**, 1650 (2010).
- ³³D. H. Dinh, L. Vellutini, B. Bennetau, C. Dejous, D. Rebière, E. Pascal, D. Moynet, C. Belin, B. Desbat, C. Labrugère, and J.-P. Pillot, *Langmuir* **25**, 5526 (2009).